Hong Kong J Radiol. 2019;22:26-31 | https://doi.org/10.12809/hkjr1916996

## ORIGINAL ARTICLE

# Correlation between Maximum Standardised Uptake Values on $^{18}$F-Fluorodeoxyglucose Positron Emission Tomography and Staging in Non-small-cell Lung Carcinoma

**KS Ng, KK Wu, KS Chu, BT Kung, TK Au Yong**

*Nuclear Medicine Unit and Clinical PET Centre, Queen Elizabeth Hospital, Jordon, Hong Kong*

## ABSTRACT

***$^{18}$F-fluorodeoxyglucose positron emission tomography–computed tomography is commonly used for the staging of non-small-cell lung carcinoma. However, few studies have investigated the correlation between the maximum standardised uptake value ($SUV_{max}$) of the primary tumour and the disease staging according to histology. The current retrospective study evaluated this relationship using statistical analyses. The findings suggest that higher $SUV_{max}$ is positively correlated with more advanced staging. This study demonstrates the importance of $SUV_{max}$ interpretation on the radiological staging of non-small-cell lung carcinoma.***

***Key Words:*** *Carcinoma, non-small-cell lung; Fluorodeoxyglucose F18; Neoplasm staging; Positron-emission tomography; Tomography, X-ray computed*

## 中文摘要

# 18氟—脱氧葡萄糖正電子攝影斷層掃描的最大標準化攝取值與非小細胞肺癌分期的相關性

**吳國勝、胡君傑、朱競新、龔本霆、歐陽定勤**

18氟—脱氧葡萄糖正電子攝影斷層掃描常用於非小細胞肺癌分期。然而，鮮有研究根據肺癌病理組織去探討原發腫瘤的最大標準化攝取值（$SUV_{max}$）與肺癌分期之間的相關性。是次回溯性研究使用統計學分析上述的相關性，結果發現$SUV_{max}$越高，肺癌分期越後。是次研究顯示$SUV_{max}$的闡釋對非小細胞肺癌的放射學分期非常重要。

## INTRODUCTION

The treatment and prognosis of non-small-cell lung carcinoma (NSCLC) heavily depends on accurate tumour, node, and metastasis (TNM) staging.[1-3] The $^{18}$F-fluorodeoxyglucose positron emission tomography–computed tomography ($^{18}$F-FDG PET-CT) is well-known for its superiority in staging NSCLC over other radiology modalities, including computed tomography

***Correspondence:*** *Dr KS Ng, Nuclear Medicine Unit and Clinical PET Centre, Queen Elizabeth Hospital, Jordon, Hong Kong. Email: ngkwoksing@gmail.com*

Submitted: 5 Jun 2018; Accepted: 26 Jun 2018.

Disclosure of Conflicts of Interest: As an editor of the journal, TK Au Yong was not involved in the peer review process. All other authors have disclosed no conflicts of interest.

Funding/Support: This research received no specific grant from any funding agency in the public, commercial, or not-for-profit sectors.

(CT)[4,5] or magnetic resonance imaging (MRI).[6,7] In addition to TNM staging, the maximum standardised uptake value ($SUV_{max}$) of the primary tumour has been suggested as a prognostic factor for postoperative mortality,[8] recurrence,[9,10] and survival.[8,11-14] However, few studies have performed statistical analyses on the correlation between $SUV_{max}$ and TNM staging. Furthermore, previous studies have typically assessed the $SUV_{max}$ irrespective of histology.[14] Yet $SUV_{max}$ depends on histology, with larger values of $SUV_{max}$ in squamous cell carcinoma (SCC) than in adenocarcinoma.[14] The aim of the current study was to clarify the relationship between the $SUV_{max}$ of the primary tumour and staging in NSCLC through statistical evaluation and subgroup analyses according to histology.

# METHODS

## Patients

In this retrospective study, patients with newly diagnosed biopsy-proven NSCLC who underwent PET-CT staging at the Nuclear Medicine Unit and Clinical PET Centre, Queen Elizabeth Hospital, Hong Kong from January 2016 to January 2017 were included. If PET-CT showed localised disease, thoracic lymph nodes were sampled by cardiothoracic surgeons or respiratory physicians within 2 months via lobectomy, mediastinoscopy, video-assisted thoracoscopic surgery, endobronchial ultrasound, pneumonectomy, or wedge resection. Histology was evaluated by pathologists according to the Mountain and Dresler scheme.[15] If PET-CT suggested distant metastases, histological or radiological investigations (including CT, MRI, bone scan, and X-ray) were supplemented to support the diagnosis of distant metastases. Patients were excluded if oncological treatment was started before PET-CT or if blood glucose was >12 mmol/L at the time of PET-CT acquisition.

## Positron Emission Tomography and Computed Tomography

The $^{18}$F-FDG PET-CT imaging was performed with a dedicated scanner (Discovery 710, General Electric, Wisconsin, US) in accordance to the 2010 procedural protocol of European Association of Nuclear Medicine for oncological PET acquisition.[16] The mean $^{18}$F-FDG activity was 10 mCi (range, 9.4-16.8 mCi). At 1 hour after $^{18}$F-FDG administration, PET imaging was acquired from skull to mid-thigh in 7 to 8 bed positions (2 min per bed position) with mean axial bed coverage of 15.7 cm per bed and 9 slices per bed overlap. The CT imaging was taken for anatomical correlation and attenuation correction with 140-kV tube voltage, 120-mA tube current, 0.5-s gantry rotation time, and 0.984 pitch. The mean blood glucose level was 5.5 mmol/L (range, 3.2-10.3 mmol/L). The PET raw data were processed using optimisation of ordered subset expectation maximisation,[17] point spread function modelling, and time-of-flight analysis (four iterations with 18 subsets and 5.5-mm cut-off frequency). The data were reconstructed with 3.27-mm slice thickness in a 256- × 256-mm matrix and processed through a standard filter. The SUV was determined by drawing regions of interest in primary tumours and then calculated with software AW Volume Viewer 4.7 (General Electric, US) according to the equation[18]:

$$SUV_{max} = \frac{Activity\ concentration_{ROI}(mCi/mL)}{Dose_{injected}(mCi)/Body\ weight\ (kg)}$$

Throughout this study, the $SUV_{max}$ of only the primary tumour was used. In case of multiple intrapulmonary tumours, the one with the highest $SUV_{max}$ was taken.

## Statistical Analyses

The $SUVs_{max}$ were categorised into three groups for analysis based on PET-CT: non-metastatic (ie, without nodal/distant metastases); nodal metastatic (ie, with biopsy-proven nodal metastasis in ipsilateral peribronchial, ipsilateral hilar, ipsilateral mediastinal or subcarinal basin but no distant metastases); and distant metastatic (ie, lung nodule in contralateral lobe, pleural nodule, pleural or pericardial effusion, or extrathoracic organs). Within each group, the $SUVs_{max}$ were further evaluated according to pathology: all histologies, adenocarcinoma, or SCC. Two-sided Student's *t* tests were performed to compare the $SUVs_{max}$ between groups.

# RESULTS

## Patient Characteristics

A total of 206 patients (144 men and 62 women; age range, 42-86 years) were analysed, with the characteristics of study population summarised in Table 1. In total, 68.4% of patients had adenocarcinoma, 19.9% had SCC, and 12.6% had other pathology (eg, adenosquamous carcinoma, poorly differentiated NSCLC, lymphoepithelioma-like carcinoma, large-cell carcinoma). In all, 26.2% of patients were included in the non-metastatic group, 17.5% in the nodal metastatic group, and 56.3% in the distant metastatic group.

## Maximum Standardised Uptake Value Analysis

Figure 1 shows typical SUV appearances in maximum intensity projection images for adenocarcinoma for

**Table 1.** Characteristics of study population (n=206).

| Characteristic | Data |
|---|---|
| Sex | |
| Male | 144 (70%) |
| Female | 62 (30%) |
| Age, mean (range), y | 66.7 (42-86) |
| Metastases | |
| Non-metastatic | 54 (26.2%) |
| Nodal metastatic | 36 (17.5%) |
| Distant metastatic | 116 (56.3%) |
| Histology* | |
| Adenocarcinoma | 141 (68.4%) |
| Non-metastatic | 38 |
| Nodal metastatic | 25 |
| Distant metastatic | 78 |
| Squamous cell carcinoma | 41 (19.9%) |
| Non-metastatic | 9 |
| Nodal metastatic | 8 |
| Distant metastatic | 24 |
| Others | 26 (12.6%) |
| Non-metastatic | 9 |
| Nodal metastatic | 3 |
| Distant metastatic | 14 |

* Two patients have double histologies.

the non-, nodal, and distant metastatic groups. Table 2 shows the mean $SUVs_{max}$ for the different groups. Variations in $SUV_{max}$ were observed even for the same stage and histology. Thus, the distribution of $SUV_{max}$ is best expressed statistically as a cumulative fraction curve against $SUV_{max}$ (ie, the number of patients in a group with $SUV_{max}$ less than the specific magnitude divided by total number of patients in the group). The cumulative fractions against $SUV_{max}$ for all histologies, only adenocarcinoma, and only SCC are shown in Figure 2.

## Group Comparison

The $SUVs_{max}$ of different groups were compared using Student's *t* test, with the corresponding p values listed in Table 3.

# DISCUSSION

A high $SUV_{max}$ for the primary tumour in NSCLC has previously been described as a poor prognostic factor for postoperative mortality,[8] disease-free survival,[9]

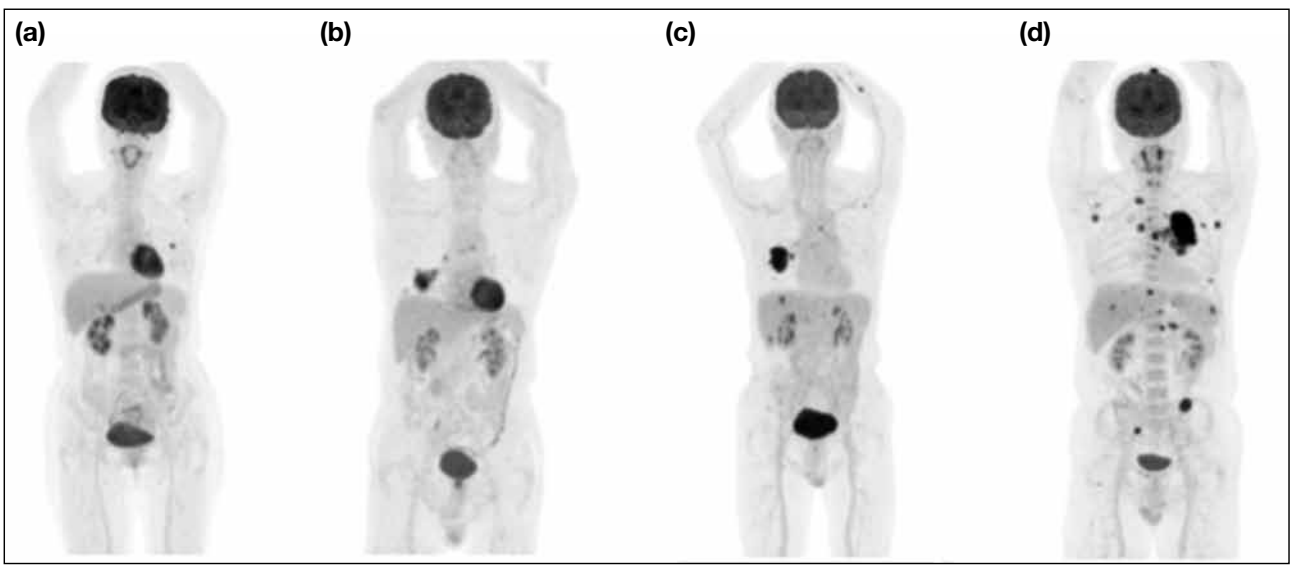


**Figure 1.** Typical maximum intensity projection images for adenocarcinoma with inverse grey colour scale: (a) non-metastatic group with primary maximum standardised uptake value ($SUV_{max}$) 7.85; (b) nodal metastatic group with $SUV_{max}$ 11.2; (c) limited distant metastatic group with $SUV_{max}$ 13.4; and (d) extensive distant metastatic group with $SUV_{max}$ 18.7. The standardised lower threshold was set at 0 and the upper threshold at 15.

**Table 2.** Maximum standardised uptake values for the non-, nodal, and distant metastatic groups, for all histologies, adenocarcinoma and squamous cell carcinoma.*

| | All histologies | Adenocarcinoma | Squamous cell carcinoma |
|---|---|---|---|
| Non-metastatic | 8.93 (7.50-10.4) | 7.01 (5.61-8.42) | 12.4 (10.3-14.6) |
| Nodal metastatic | 10.9 (9.46-12.3) | 10.0 (8.46-11.6) | 12.4 (8.65-16.1) |
| Distant metastatic | 13.2 (12.1-14.3) | 12.4 (11.3-13.5) | 16.8 (13.2-20.2) |

* Data are shown as mean (95% confidence interval).

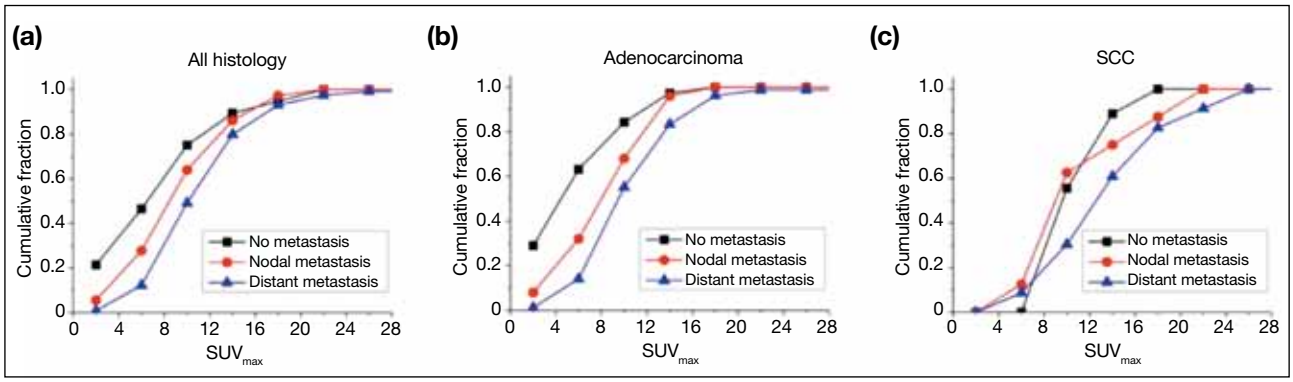


**Figure 2.** Cumulative fraction against maximum standardised uptake value ($SUV_{max}$) plot for (a) all histologies, (b) adenocarcinoma and (c) squamous cell carcinoma (SCC). The lines represent the non-metastatic group (black squares), nodal metastatic group (red circles), and distant metastatic group (blue triangles).

**Table 3.** P values of two-tailed Student's *t* tests in the comparisons of non-metastatic versus nodal metastatic, nodal versus distant metastatic, and adenocarcinoma versus squamous cell carcinoma groups, with subgroup analyses as listed.

| Comparison | Subgroup | p Value |
|---|---|---|
| Non-metastatic vs nodal metastatic | All histology | 0.0182 |
| | Adenocarcinoma | 0.0058 |
| | Squamous cell carcinoma | 0.97 |
| Nodal metastatic vs distant metastatic | All histology | 0.0242 |
| | Adenocarcinoma | 0.0346 |
| | Squamous cell carcinoma | 0.167 |
| Adenocarcinoma vs squamous cell carcinoma | Non-metastatic | 0.0008 |
| | Nodal metastatic | 0.16 |
| | Distant metastatic | 0.0023 |

recurrence,[9,10] and distant metastases-free survival.[10] However, few studies have provided statistical analysis of $SUV_{max}$ between non-, nodal, and distant metastatic groups. In addition, few studies have evaluated $SUV_{max}$ according to histology. Histology-based $SUV_{max}$ analysis is important; the results of the current study show that the $SUV_{max}$ for SCC is greater than that of adenocarcinoma, consistent with the literature.[14] The current study also shows that more advanced disease is correlated with greater $SUV_{max}$. Qualitative examples, such as the maximum intensity projection images shown in Figure 1, indicate that primary tumours have a greater uptake for more aggressive disease. Even for the distant metastatic group, $SUV_{max}$ was greater for more extensive metastases, as shown in Figure 1c and d. Quantitative analyses in Figure 2 and Table 3 verify that $SUV_{max}$ rank highest for the distant, followed by nodal and non-metastatic groups for all histologies and adenocarcinoma, with $p<0.05$. For example, Figure 2b shows that only 17% of non-metastatic adenocarcinoma have $SUV_{max}$ >10, whereas 35% of nodal and 50% of distant metastatic adenocarcinoma have $SUV_{max}$ >10. This finding has an important clinical implication: high $SUV_{max}$ should raise clinician's suspicion of nodal or distant metastases. Figure 3a shows the maximum intensity projection image of a patient newly diagnosed with adenocarcinoma of lung. Two hypermetabolic nodules are noted over the right upper lobes ($SUV_{max}$ 15.6 and 4.1), together with a mildly hypermetabolic right interlobar lymph node. Otherwise, there is no definite evidence of distant metastases from skull base to mid-thigh. In view of the radiological T3N1 disease, radical surgery may be offered. However, for the non- and nodal metastatic groups, only 5% have primary $SUV_{max}$ ≥15.6, whereas for the metastatic group, 20% have primary $SUV_{max}$ ≥15.6 (Figure 2b). Thus, distant metastases should be suspected of in view of the high $SUV_{max}$. A common metastatic site of lung adenocarcinoma is in the brain, which may be missed in PET-CT. For this patient, brain MRI was offered, revealing multiple cerebral metastases (representative image in Figure 3b). The patient subsequently received palliative

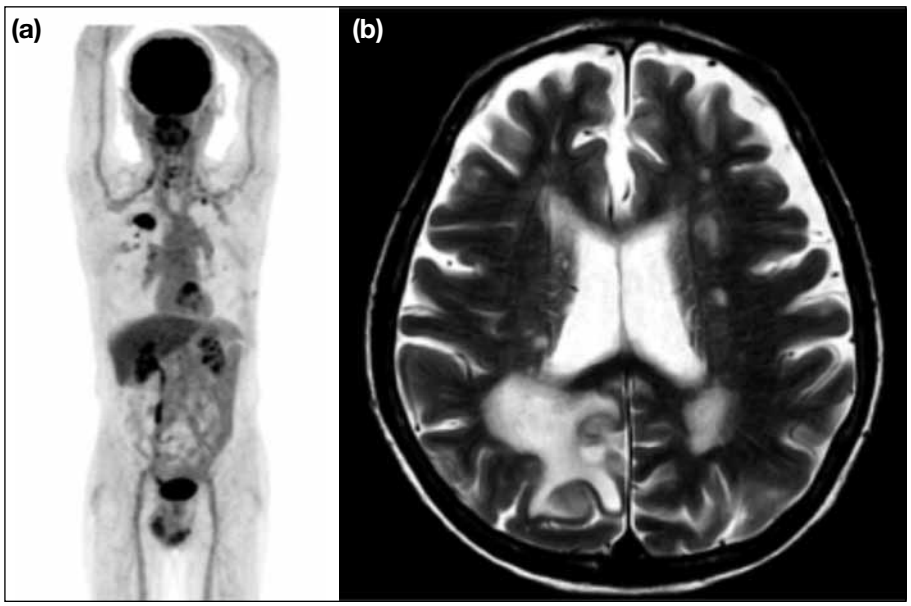


**Figure 3.** (a) Maximum intensity projection image of a patient with newly diagnosed adenocarcinoma. Two hypermetabolic nodules with the maximum standardised uptake values of 15.6 and 4.1 in the right upper lobes and a hypermetabolic right interlobar lymph node are noted. No suspicious hypermetabolic lesion elsewhere suggestive of distant metastases. The standardised lower threshold was set at 0 and the upper threshold at 5. (b) Representative T2-weighted magnetic resonance image of the same patient shows a hyperintense lesion in the right parietal lobe, together with surrounding oedema suggestive of intracranial metastasis.

radiotherapy and chemotherapy. This example illustrates the importance of interpreting high $SUV_{max}$. In contrast, low $SUV_{max}$ magnitude implies a lower likelihood for nodal or distant metastases. Figure 4a shows the maximum intensity projection image of another patient with two hypermetabolic nodules at right lower and upper lobes ($SUVs_{max}$ of 7.8 and 7.0), without definite evidence of nodal or distant metastases. The differentials include double primaries or intrapulmonary metastases. Correct radiological staging is critical here to determine if treatment intent is curative or palliative. Although certain morphological features may help distinguish the two differentials, the features have significant overlap between different histological types.[19] The current study suggests that a tumour with a low $SUV_{max}$ is less likely than a tumour with a high $SUV_{max}$ to have nodal or distant involvement. Based on Figure 2b, primary $SUV_{max}$ is ≤7 in 70% of non-metastatic adenocarcinoma, but in only 20% of distant metastatic adenocarcinoma. Thus, the radiological findings suggest double primaries. The patient eventually underwent radical right upper and lower lobe lobectomy. Final pathology confirmed this diagnosis, with one lesion having wild-type epidermal growth factor receptor and the other mutated epidermal growth factor receptor. The results of the current study show that $SUV_{max}$ interpretation is also important for risk stratification of nodal and distant metastasis. Figure 2b indicates that, for example, 80% risks in nodal and distant metastasis correspond to $SUV_{max}$ cut-offs of 12 and 14, respectively. However, exact $SUVs_{max}$ depend on many factors.[20]

**Figure 4.** Maximum intensity projection image of a patient with two hypermetabolic nodules at the right lower and upper lobes, with corresponding maximum standardised uptake values of 7.8 and 7.0. The standardised lower threshold was set at 0 and the upper threshold at 5.

For SCC, the results of current study show that the distant metastatic group generally has higher $SUV_{max}$ than non- and nodal metastatic groups (Table 2 and Figure 2c). However, the differences are not statistically significant (p=0.97 for non-metastatic compared with nodal metastatic groups; p=0.167 for nodal metastatic

compared with distant metastatic groups), probably owing to the low number of SCC cases included compared with all histologies and adenocarcinoma (41 vs 206 and 141, respectively; Table 1).

A previous study suggested that the $SUV_{max}$ in SCC is generally higher than that in adenocarcinoma, although corresponding disease extent was not well clarified.[21] The findings of the current study suggest that $SUV_{max}$ depends on the disease extent. Our study also confirms that the $SUV_{max}$ in SCC is higher than that in adenocarcinoma for the non-, nodal, and distant metastatic groups (Tables 2 and 3). However, the difference in the nodal group was not statistically significant (p=0.16), likely owing to the low number of SCC cases.

## CONCLUSION

The current retrospective study investigated the $SUV_{max}$ of primary NSCLC tumours. The $SUV_{max}$ was found to be dependent on TNM staging, and was highest in the distant metastatic group and lowest in the non-metastatic group. The application of $SUV_{max}$ interpretation to radiological staging was demonstrated through examples.

## REFERENCES


1. Spira A, Ettinger DS. Multidisciplinary management of lung cancer. N Engl J Med. 2004;350:379-92. Crossref
2. Ettinger DS, Wood DE, Aisner DL, Akerley W, Bauman J, Chirieac LR, et al. Non-small cell lung cancer, version 5.2017, NCCN Clinical Practice Guidelines in Oncology. J Natl Compr Canc Netw. 2017;15:504-35. Crossref
3. Edge SB, Compton CC. The American Joint Committee on Cancer: the 7th edition of the AJCC cancer staging manual and the future of TNM. Ann Surg Oncol. 2010;17:1471-4. Crossref
4. Hellwig D, Graeter TP, Ukena D, Groeschel A, Sybrecht GW, Schaefers HJ, et al. $^{18}$F-FDG PET for mediastinal staging of lung cancer: which SUV threshold makes sense? J Nucl Med. 2007;48:1761-6. Crossref
5. Bryant AS, Cerfolio RJ. The maximum standardized uptake values on integrated FDG-PET/CT is useful in differentiating benign from malignant pulmonary nodules. Ann Thorac Surg. 2006;82:1016-20. Crossref
6. Webb WR, Sarin M, Zerhouni EA, Heelan RT, Glazer GM, Gatsonis C. Interobserver variability in CT and MR staging of lung cancer. J Comput Assist Tomogr. 1993;17:841-6. Crossref
7. Kernstine KH, Stanford W, Mullan BF, Rossi NP, Thompson BH, Bushnell DL, et al. PET, CT, and MRI with Combidex for mediastinal staging in non-small cell lung carcinoma. Ann Thorac Surg. 1999;68:1022-8. Crossref
8. Jeong HJ, Min JJ, Park JM, Chung JK, Kim BT, Jeong JM, et al. Determination of the prognostic value of [18F] fluorodeoxyglucose uptake by using positron emission tomography in patients with non-small cell lung cancer. Nucl Med Commun. 2002;23:865-70. Crossref
9. Cerfolio RJ, Bryant AS, Ohja B, Bartolucci AA. The maximum standardized uptake values on positron emission tomography of a non-small cell lung cancer predict stage, recurrence, and survival. J Thorac Cardiovasc Surg. 2005;130:151-9. Crossref
10. Sasaki R, Komaki R, Macapinlac H, Erasmus J, Allen P, Forster K, et al. SUV by FDG-PET predicts outcome of non-small cell lung cancer. Intl J Radiat Oncol. 2003;57:S166. Crossref
11. Higashi K, Ueda Y, Arisaka Y, Sakuma T, Nambu Y, Oguchi M, et al. 18F-FDG uptake as a biologic prognostic factor for recurrence in patients with surgically resected non-small cell lung cancer. J Nucl Med. 2002;43:39-45.
12. Vansteenkiste JF, Stroobants SG, Dupont PJ, De Leyn PR, Verbeken EK, Deneffe GJ, et al. Prognostic importance of the standardized uptake value on (18)F-fluoro-2-deoxy-glucose-positron emission tomography scan in non-small-cell lung cancer: an analysis of 125 cases. J Clin Oncol. 1999;17:3201-6. Crossref
13. Ahuja V, Coleman RE, Herndon J, Patz EF Jr. The prognostic significance of fluorodeoxyglucose positron emission tomography imaging for patients with nonsmall cell lung carcinoma. Cancer. 1998;83:918-24. Crossref
14. Downey RJ, Akhurst T, Gonen M, Vincent A, Bains MS, Larson S, et al. Preoperative F-18 fluorodeoxyglucose-positron emission tomography maximal standardized uptake value predicts survival after lung cancer resection. J Clin Oncol. 2004;22:3255-60. Crossref
15. Mountain CF, Dresler CM. Regional lymph node classification for lung cancer staging. Chest. 1997;111:1718-23. Crossref
16. Boellaard R, O'Doherty MJ, Weber WA, Mottaghy FM, Lonsdale MN, Stroobants SG, et al. FDG PET and PET/CT: EANM procedure guidelines for tumour PET imaging: version 1.0. Eur J Nucl Med Mol Imaging. 2010;37:181-200. Crossref
17. Hudson HM, Larkin RS. Accelerated image reconstruction using ordered subsets of projection data. IEEE Trans Med Imaging. 1994; 13:601-9. Crossref
18. Nabi HA, Zubeldia JM. Clinical applications of (18)F-FDG in oncology. J Nucl Med Technol. 2002;30:3-9.
19. Lindell RM, Hartman TE, Swensen SJ, Jett Jr, Midthun DE, Tazelaar HD, et al. Five-year lung cancer screening experience: CT appearance, growth rate, location, and histologic features of 61 lung cancers. Radiology. 2007;242:555-62. Crossref
20. Boellaard R. Standards for PET image acquisition and quantitative data analysis. J Nucl Med. 2009;50 Suppl 1:11S-20S. Crossref
21. Aquino SL, Halpern EF, Kuester LB, Fischman AJ. FDG-PET and CT features of non-small cell lung cancer based on tumor type. Int J Mol Med. 2007;19:495-9. Crossref